Electronic Supplementary Material (ESI) for Materials Advances.

Supporting Information

$Cs_2Ag_xNa_{1-x}Bi_yIn_{1-y}Cl_6$ Perovskites Approaching Photoluminescence Quantum Yields of 100 %

Oleksandr Stroyuk[1*], Oleksandra Raievska[1], Anastasia Barabash[2], Christian Kupfer[2], Andres Osvet[2], Volodymyr Dzhagan[3,4], Dietrich R.T. Zahn[5,6] Jens Hauch[1,2], Christoph J. Brabec[1,2]

[1]*Forschungszentrum Jülich GmbH, Helmholtz-Institut Erlangen Nürnberg für Erneuerbare Energien (HI ERN), 91058 Erlangen, Germany*

[2]*Friedrich-Alexander-Universität Erlangen-Nürnberg, Materials for Electronics and Energy Technology (i-MEET), Martensstrasse 7, 91058 Erlangen, Germany*

[3]*V. Lashkaryov Institute of Semiconductors Physics, National Academy of Sciences of Ukraine, 03038 Kyiv, Ukraine*

[4]*Physics Department, Taras Shevchenko National University of Kyiv, 60 Volodymyrs'ka str., 01601 Kyiv, Ukraine*

[5]*Semiconductor Physics, Chemnitz University of Technology, 09107 Chemnitz, Germany*

[6]*Center for Materials, Architectures and Integration of Nanomembranes (MAIN), Chemnitz University of Technology, 09107, Chemnitz, Germany*

Authors for correspondence:

[*]Dr. Oleksandr Stroyuk, Forschungszentrum Jülich GmbH, Helmholtz-Institut Erlangen Nürnberg für Erneuerbare Energien (HI ERN), Immerwahrstr. 2, 91058 Erlangen, Germany; *e-mail*: o.stroyuk@fz-juelich.de, alstroyuk@ukr.net.

1. Synthesis

$Cs_2Ag_xNa_{1-x}InCl_6$ (CANIC), $Cs_2Ag_xNa_{1-x}Bi_yIn_{1-y}Cl_6$ (CANBIC), and $Cs_2Ag_xNa_{1-x}BiCl_6$ (CANBC) perovskites were synthesized at room temperature in ambient atmosphere via a combination of two precursor solutions in 2-propanol:water mixtures, one of them containing a minimal amount of HCl to prevent hydrolytic reactions of Bi^{3+} and In^{3+} ions.

A stock $BiCl_3$ solution (1.0 M) was first prepared in 4.0 M HCl. This acid concentration is the lowest one, at which $BiCl_3$ is dissolved completely without forming a precipitate due to hydrolysis. In a similar manner, a stock $InCl_3$ solution (1.0 M) in 4.0 M HCl was prepared.

For the synthesis of perovskites two precursor solutions were prepared separately as described below and then solution I was mixed with solution II under vigorous stirring and the sample was kept at least 300 min at ambient conditions before the purification to reach deeper crystallization.

Precursor solution I was prepared by adding to a beaker *N* mL (A = 0 – 1.0) stock 1.0 M $BiCl_3$ solution in 4.0 M HCl, 1-*N* mL 1.0 M stock $InCl_3$ solution in 4.0 M HCl, 1.0 mL concentrated 37 w.% (12 M) HCl, and 5 mL 2-propanol. The acid can be mixed with 2-propanol beforehand to avoid HCl evaporation and used as a single reactant.

Precursor solution II was prepared by mixing 5 mL 2-propanol with 1.0 mL deionized (DI) water, 0.4 mL aqueous 1.0 M $AgNO_3$ solution, and 0.25 mL aqueous 5.0 M ammonia solution in a beaker placed on a magnetic stirrer. Ammonia was added to form an Ag(I)-NH_3 complex and avoid formation of silver hydroxide upon interaction with alkaline solutions of Cs(I) and Na(I) acetates. Afterwards, 0.25 mL 4.0 M aqueous NaAc (Ac = acetate) and 0.6 mL aqueous 4.0 M CsAc solutions were added at intense stirring. Both precursor solutions remained transparent and colorless till the final mixing.

Note: for the preparation of stock solutions with the concentration of 1.0 M and higher the precursor salts should be dissolved in a minimal amount of solvent and then pure solvent added till the final calculated volume of the solution is reached, to account for the volume of the dissolved salts which cannot be neglected in the case of such concentrations.

Purification. Mixing of the two starting solutions resulted in the formation of a white precipitate, which was stable for many days when kept in the supernatant due to the presence of excess Na and Cs ions. To purify the perovskite, it was separated from the supernatant, 10 mL pure 2-propanol were added to the precipitate and the mixture was subjected to centrifugation at 3000 rpm for 3 min. Then the precipitate was separated again, and the procedures of 2-propanol addition and centrifugation were repeated. The CANBIC powders were dried at room

temperature and kept in vials under ambient conditions. The mass yield of the synthesis was 0.5-0.7 g depending on the CANBIC composition.

Formation of samples for optical and structural studies. Homogeneous samples on substrates were produced from fresh precipitates. Glass or adhesive carbon tape on silicon were used as substrates for optical characterization, X-ray diffraction (XRD), and scanning electron microscopy/energy-dispersive X-ray spectroscopy (SEM/EDX), respectively. To produce the samples, 0.20 mL 2-propanol is added to 50 mg of freshly synthesized and purified precipitate, mixed till the formation of a homogeneous suspension and deposited on the substrates by drop-casting. The suspension covers the substrate spontaneously and can be left for drying for 2-5 min under ambient conditions forming a dense and homogeneous layer.

2. Characterization methods

Spectral characterization. Reflectance spectra were recorded using a BlackComet spectrometer (StellarNet Inc.) and a 75W Xenon lamp (Thorlabs) as an excitation source. The spectra were registered with an optical Y-fiber probe in identical geometry for samples and a reference (ultra-pure $BaSO_4$, Alfa-Aesar). Absorption spectra were then calculated by dividing the reflectance spectra of the sample and the reference and subtracting the baseline. Additionally, absorption spectra were recorded for CANBIC during PL QY measurements using a Quantaurus spectrometer. These spectra were identical to those detected using the BlackComet spectrometer.

Absolute PL QYs were determined using a Quantaurus-QY spectrometer (Hamamatsu) at room temperature. The sample was excited by the light from an in-built Xenon lamp with an excitation wavelength selected using a monochromator with 5 nm spectral width. Ultra-pure $BaSO_4$ samples from Alfa-Aesar, Sigma-Aldrich, and ThermoFisher were used as scattering references, all producing identical results. Four independently synthesized samples with the same composition were measured with a set of excitation wavelengths and a distribution of PL QY values plotted to determine the average PL QY and standard deviation of the measurement. PL excitation and absorption spectra were additionally produced during these measurements.

PL spectra were registered similarly to the reflectance spectra using a BlackComet spectrometer in the range of 190-1000 nm using a UV LED (360-370 nm, Thorlabs) as an excitation source. The PL spectra were found to be identical to those registered during PL QY measurements using the Quantaurus spectrometer.

Photographs of luminescent CANBIC perovskites were registered at ambient conditions under illumination with an UV lamp (350-370 nm).

Kinetic curves of PL decay were registered using a custom-designed setup based on a FluoTime300 luminescence spectrometer (Picoquant) equipped with 402 nm LDH-P-C-405B laser. The samples were excited by the 402 nm laser using an optical fiber and the PL signal was collected in the range of 420-800 nm with excitation and emission slits set to 4 nm. In the case of temperature-dependent time-resolved PL measurements the samples were placed in an Oxford Instruments cryostat, which was optically coupled to the spectrometer.

Raman spectra were excited using a 514.7 nm diode pumped solid state (DPSS) laser (Cobolt) and registered at a spectral resolution of about 2 cm^{-1} using a LabRam HR800 micro-Raman system equipped with a liquid nitrogen cooled CCD detector. The incident laser power under the microscope objective (50x) was in the range of 0.1 - 0.001 mW.

Structural characterization. XRD patterns were registered using a Panalytical X'pert powder diffractometer with filtered Cu K_α radiation (λ = 1.54178 Å) and an X'Celerator solid-state stripe detectorin the Bragg-Brentano geometry in an angle range of 2θ = 5-100° with a step rate of 0.05° per min. The samples were drop-casted as suspensions in 2-propanol on glass substrates and dried at ambient conditions. The XRD patterns were subjected to a Rietvield refinement procedure using MAUD software.

SEM and cathodoluminescence imaging as well as EDX analysis were performed using a JEOL JSM-7610F Schottky field emission scanning electron microscope operating under 15-20 kV acceleration voltage. equipped with Deben Centaurus detector (for CL measurements) and X-Max 80 mm^2 silicon drift detector (Oxford Instruments and AZtec nanoanalysis software, for EDX measurements). The samples were prepared by drop-casting a suspension in 2-propanol on adhesive carbon tape placed on top of a single silicon crystal and dried at ambient conditions.

XPS measurements were performed with an ESCALAB 250Xi X-ray Photoelectron Spectrometer (Thermo Scientific) equipped with a monochromatic Al K_α (1486.7 eV) source. A pass energy of 200 eV was used for survey spectra and 20 eV for high-resolution core-level spectra (providing a spectral resolution of 0.5 eV). Spectra deconvolution and quantification were performed using the Avantage Data System (Thermo Scientific).

3. Calculation of rate constants of radiative and non-radiative recombination

By combining stationary measurements of the PL QY with the kinetic data on PL lifetime the values of the rate constants of the radiative recombination k_r and the non-radiative recombination k_{nr} can be calculated. The radiative lifetime is inversely proportional to the sum of the rate constants of all recombination routes (eq. (1)), while the PL QY represents the fraction of the radiative channels in the entire set of recombination events (eq. (2)). By combining eq. (1) and (2) we can evaluate the radiative recombination rate constant (eq. (3)) and then calculate the rate constant of the non-radiative recombination processes.

$$\tau = \frac{1}{k_r + k_{nr}} \qquad (1)$$

$$\mathrm{PLQY} = \frac{k_r}{k_r + k_{nr}} \qquad (2)$$

$$k_r = \frac{\mathrm{PLQY}}{\tau} \qquad (3)$$

4. Supplementary figures

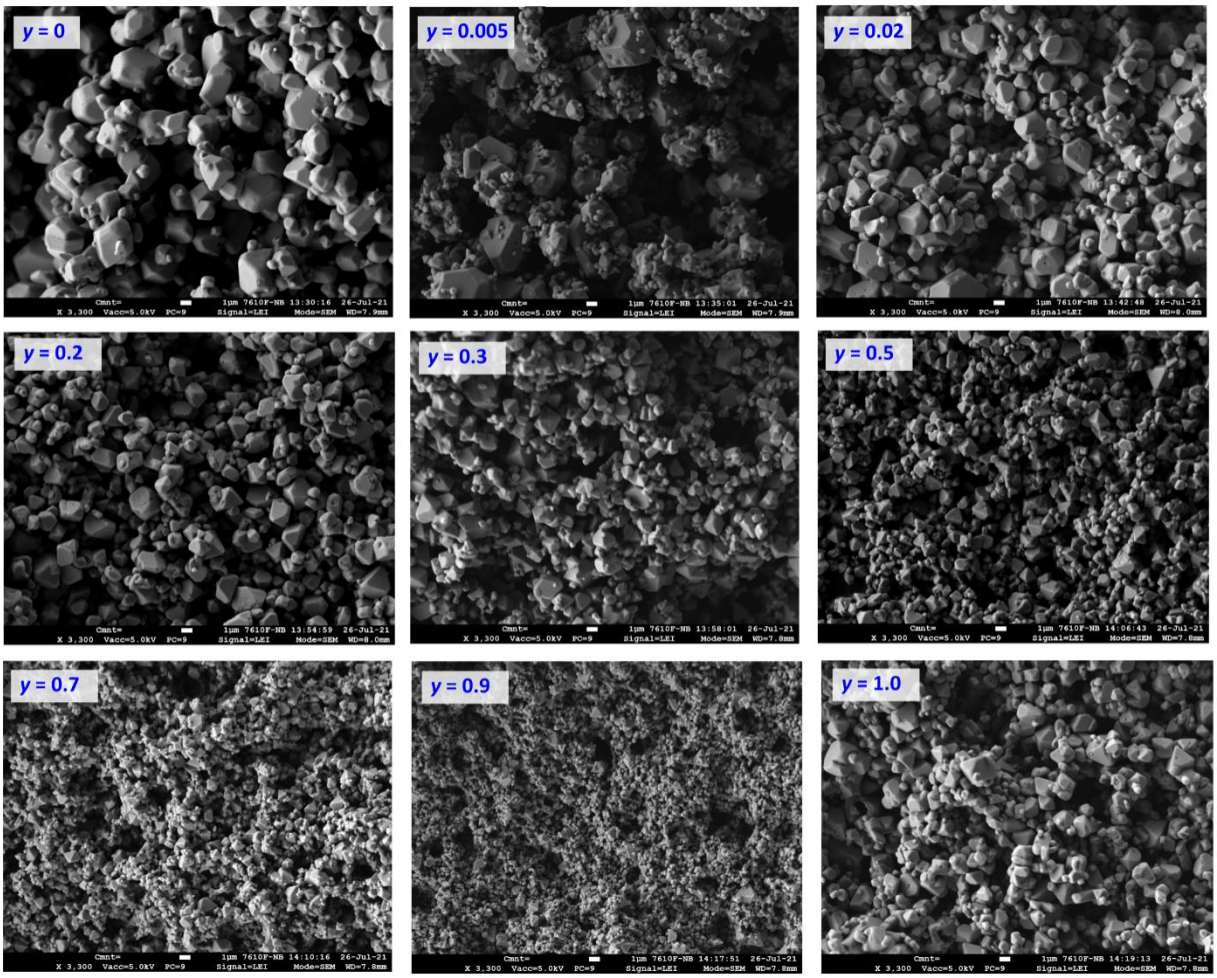

Figure S1. SEM images of CANBIC perovskites with varied Bi fraction *y*. Scale bar is 1 μm.

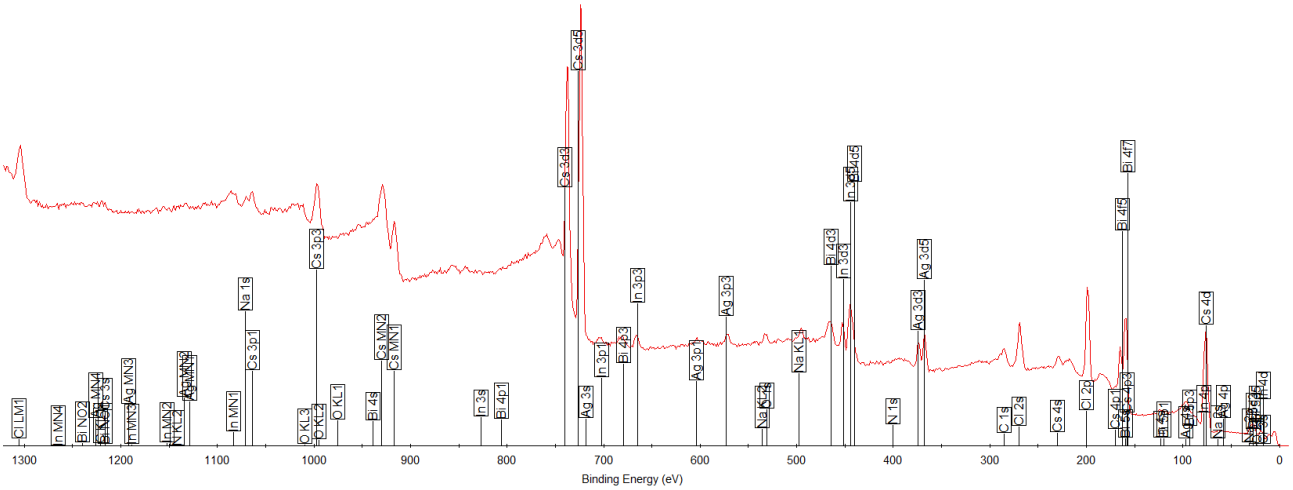

Figure S2. Exemplary X-ray survey photoelectron spectrum of a CANBIC sample (y = 0.02) with element peak positions identified by Avantage Data System (Thermo Scientific).

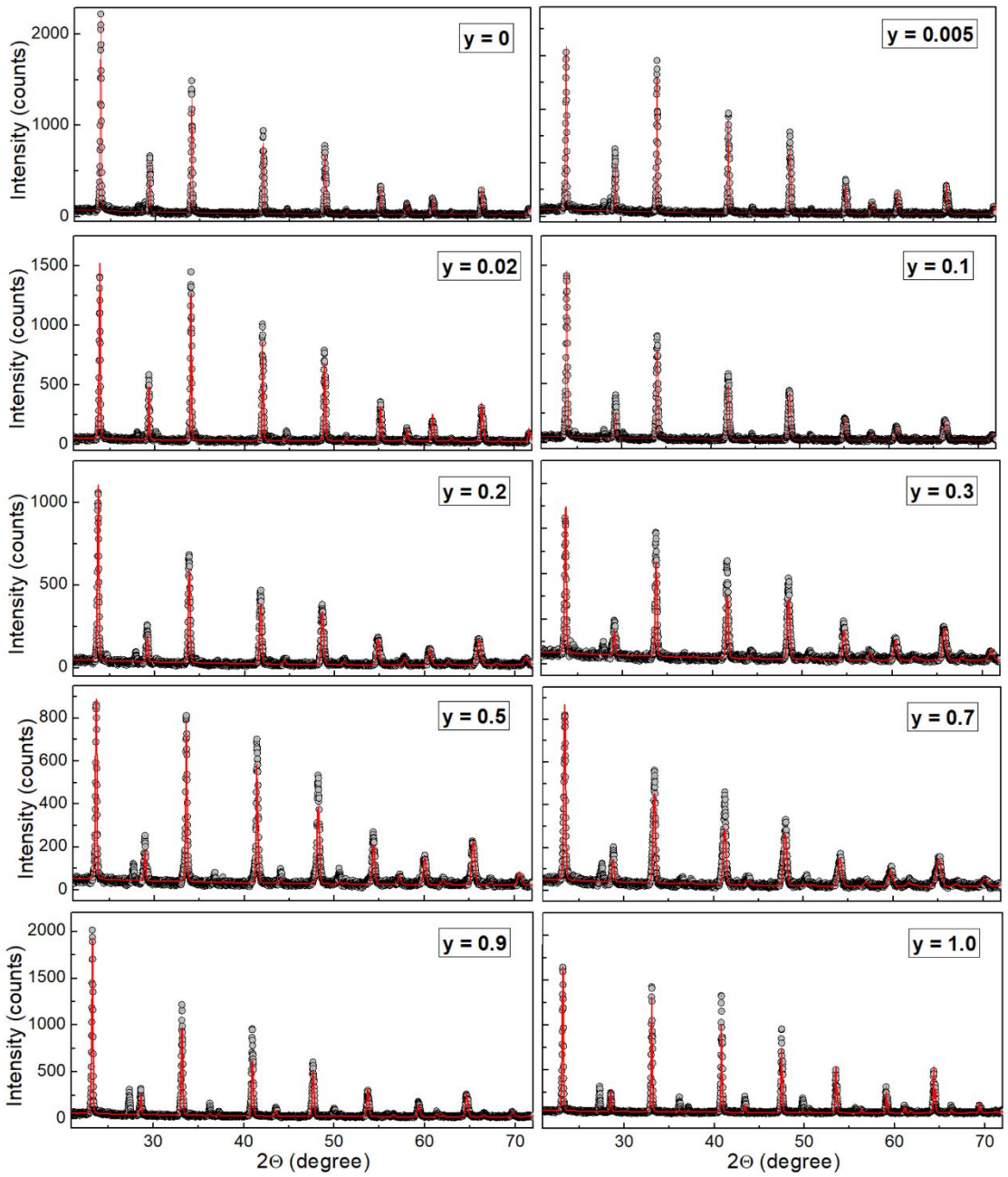

Figure S3. XRD patterns of CANBIC perovskites with varied Bi fraction *y*. Gray circles represent experimental data, red solid lines the Rietvield refinement analysis.

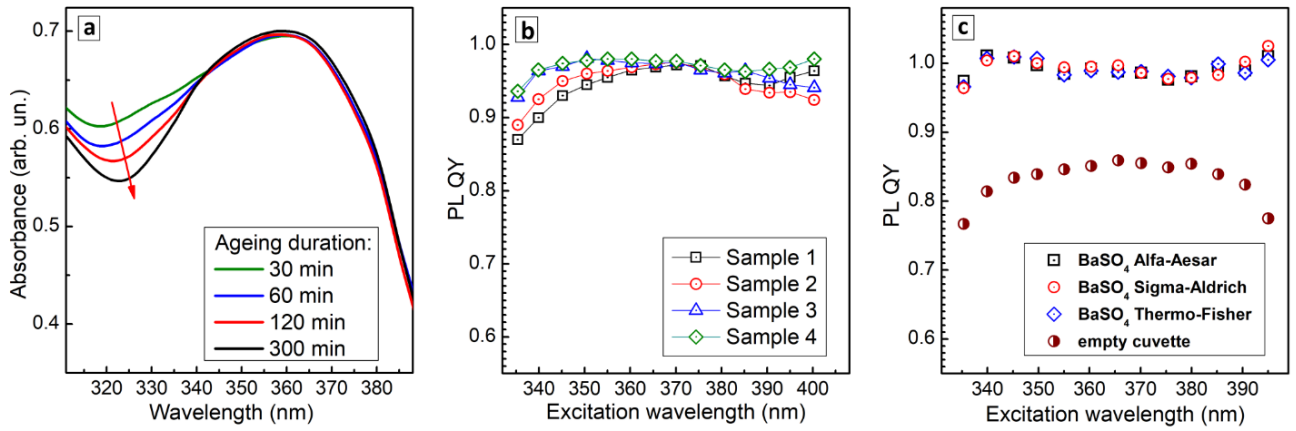

Figure S4. (a) Absorption spectra of CANBIC-2% perovskite registered at different duration of ageing in the parental solution varied from 30 to 300 min. (b) PL QYs measured at RT for four identical CANBIC-2% samples synthesized independently at different excitation wavelengths. (c) PL QYs measured at RT for a CANBIC-1% perovskite using three different samples of ultra-pure $BaSO_4$ as well as empty cuvette as a reference. The manufacturers of the $BaSO_4$ samples are given in the figure.

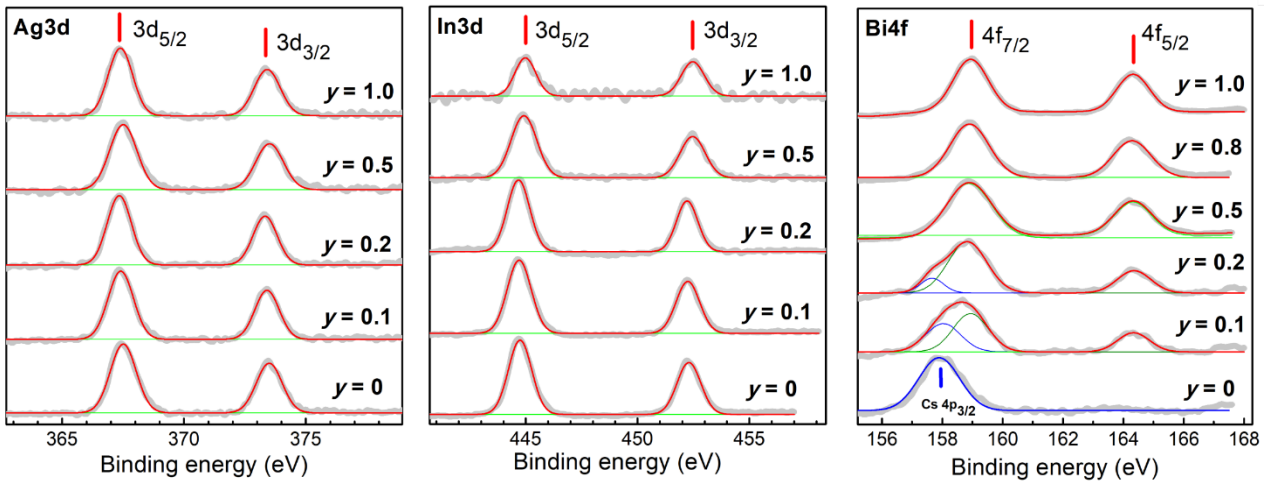

Figure S5. High-resolution X-ray photoelectron spectra of CANBIC perovskites with varied Bi fraction *y* in the range of Ag3d, In3d, and Bi4f electron binding energies. Gray curves represent experimental spectra, red and blue lines the fits with Gaussian profiles.

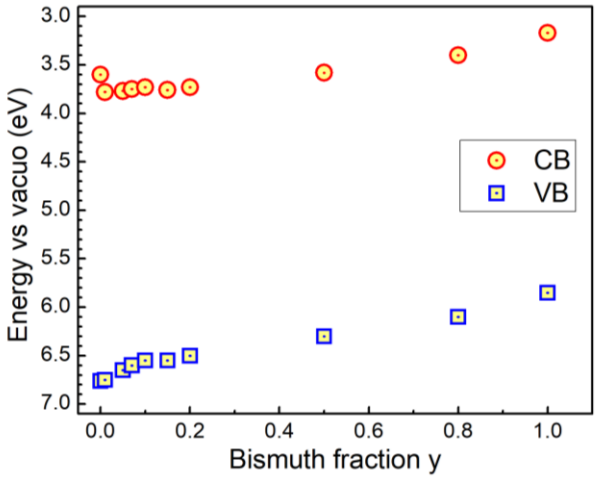

Figure S6. VB and CB levels of CANBIC perovskites as a function of Bi fraction y estimated from X-ray photoelectron spectra.

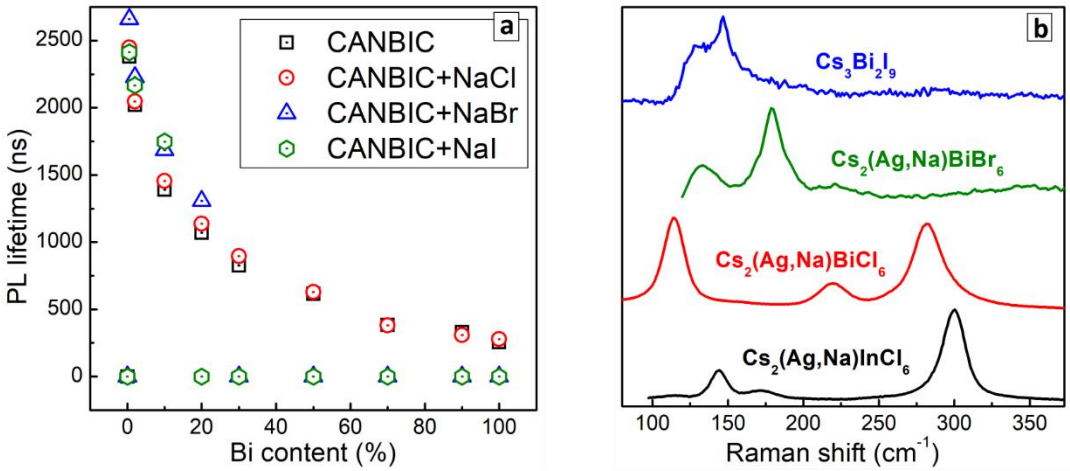

Figure S7. (a) PL lifetime as a function of the molar Bi fraction *y* for CANBIC perovskites with no treatments (squares), and treated with NaCl (circles), NaBr (triangles), and NaI (diamonds). (b) Representative Raman spectra of CANIC, CANBC, CABB, and CBI perovskites.

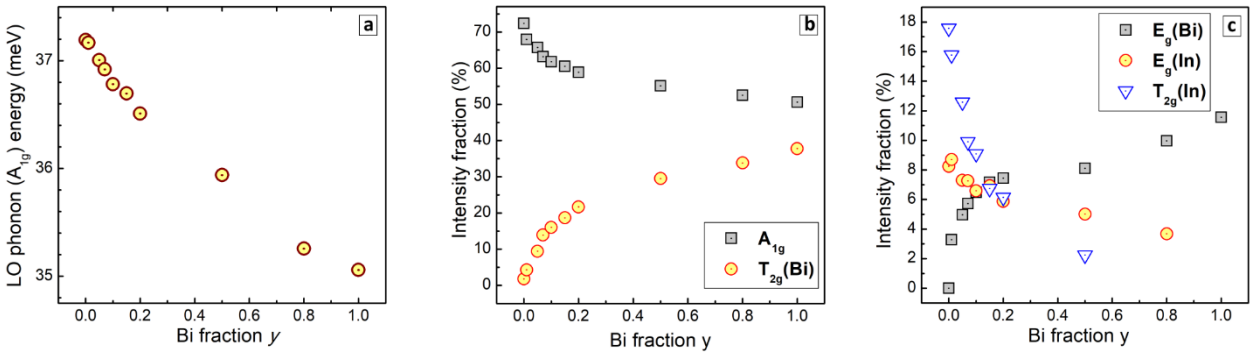

Figure S8. Energy of LO phonon (a) and partial intensities of different vibrational modes (b,c) as functions of the Bi fraction *y*.

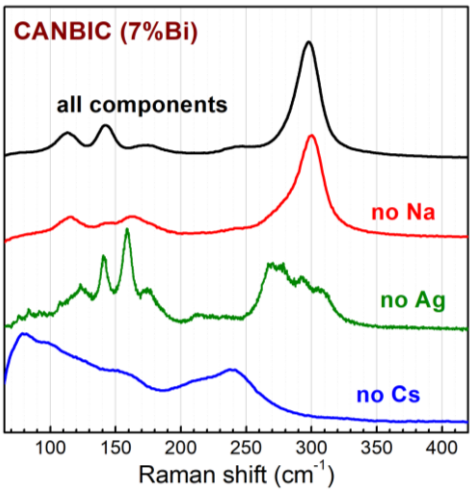

Figure S9. Selected Raman spectra of CANBIC-7% perovskite produced in normal conditions as well as in the absence of Na, Ag, and Cs.

5. Supplementary tables

Table S1. Elemental composition of CANBIC perovskites with nominal *x* = 0.4 and varied Bi content identified by survey XPS measurements

Nominal *y*	Cs, at.%	Na, at.%	Ag, at.%	In, at.%	Bi, at.%	Cl, at.%	Real *y*	Real *x*	Cl-to-M ratio
0	25.0	5.0	4.0	9.0	0	57.0	0	0.44	6.3
0.01	25.8	4.5	3.5	9.0	0.2	57.0	0.02	0.44	6.2
0.05	25.0	5.0	3.5	8.5	0.5	57.5	0.06	0.41	6.4
0.07	25.0	5.0	3.2	9.0	0.8	57.5	0.08	0.39	5.9
0.10	25.0	5.0	3.8	8.0	1.0	57.2	0.11	0.43	6.4
0.15	25.0	5.0	4.1	7.6	1.3	57.0	0.15	0.45	6.4
0.20	25.2	5.2	3.5	6.8	2.1	57.2	0.24	0.40	6.4
0.50	26.0	5.1	3.3	4.3	4.2	57.1	0.48	0.39	6.7
0.80	26.0	5.0	3.6	1.9	6.2	57.3	0.76	0.42	7.1
1.00	26.4	5.2	4.3	0	7.4	56.7	1.00	0.45	7.7

Table S2. Binding energies for Bi^{3+} in different CANBICs

y	Bi4f7/2	Bi4f5/2	In3d5/2	In3d3/2	Ag3d5/2	Ag3d3/2
0	-	-	444.7	452.3	367.5	373.5
0.1 (5)	158.9	164.3	444.7	452.2	367.4	373.4
0.2 (7)	158.9	164.4	444.7	452.2	367.3	373.3
0.5 (8)	158.9	164.3	444.9	452.5	367.5	373.5
0.8 (9)	158.9	164.3	445.0	452.5	367.4	373.4
1.0 (10)	158.9	164.3	-	-	367.5	373.5

Table S3. Bandgaps, VB and CB levels of CANBIC perovskites with varied Bi fraction *y*

y	E_g (eV)	VB energy vs E_F (eV)	CB energy vs E_F (eV)	VB energy vs vacuo (eV)	CB energy vs vacuo (eV)
0	3.16	2.66	-0.50	6.76	3.6
0.01	2.97	2.65	-0.32	6.75	3.78
0.05	2.88	2.55	-0.33	6.65	3.77
0.07	2.85	2.5	-0.35	6.6	3.75
0.10	2.82	2.45	-0.37	6.55	3.73
0.15	2.79	2.45	-0.34	6.55	3.76
0.20	2.77	2.4	-0.37	6.5	3.73
0.50	2.72	2.2	-0.52	6.3	3.58
0.80	2.7	2.0	-0.70	6.1	3.4
1.00	2.68	1.75	-0.93	5.85	3.17